Finite Element Modeling of Temperature Evolution During Selective Laser Melting

Nithya Srimurugan, Rishi Dwivedi, Vineesh Vishnu, Basil Kuriachen, and K. P. Vineesh

1 Introduction

Additive manufacturing is a direct production process in which the components are made from a 3D model using layer by layer deposition. Additive manufacturing has emerged as a widely accepted technique in aerospace, automotive, medical, and food industries owing to its capabilities of making net-shaped complex geometries, better properties, no wastage of material, and less production time compared to the conventional manufacturing methods. Powder bed fusion is a promising metal additive manufacturing method that utilizes various printing techniques such as Selective Laser Melting (SLM), Electron Beam Melting (EBM), Direct Metal Laser Sintering (DMLS), and Selective Laser Sintering (SLS). The SLM technique uses a high-power density laser with a large thermal gradient to melt and fuse the metallic powders and a rapid cooling cycle to solidify the part in an inert atmosphere. Despite many advantages, SLM parts also suffer some defects include porosity, lack of fusion, and tensile residual stresses. The defects finally cause the formation of cracks in the printed parts and change in the part dimension and shape. The balling effect, tensile residual stresses, and deteriorated surface finish, and localized thermal stresses are detrimental to the acceptability of the parts for heavy-duty applications [1, 2]. Various researchers focused their studies on residual stresses and part deformation during the SLM process [3, 4]. Experimental techniques employed to measure the temperature field and the residual stresses are very expensive and time-consuming [5]. Accurate prediction of residual stress depends on the temperature field distribution during the melting operation. To study the evolution of temperature in the SLM process, an effective modeling is required.

N. Srimurugan (✉) · R. Dwivedi · V. Vishnu · B. Kuriachen · K. P. Vineesh
Department of Mechanical Engineering, National Institute of Technology Calicut, Calicut 673601, India

© The Author(s), under exclusive license to Springer Nature Singapore Pte Ltd. 2022

S. K. Natarajan et al. (eds.), *Recent Advances in Manufacturing, Automation, Design and Energy Technologies*, Lecture Notes in Mechanical Engineering,
https://doi.org/10.1007/978-981-16-4222-7_37

Roberts et al. [6] developed a 3D finite element model without radiation heat transfer loss and predicted the temperature field during the SLM of Ti6Al4V alloy. In another study, Li et al. [7] predicted the optimum process parameters needed for a sound metallurgical bonding for AlSi10Mg alloy with the help of a 3D FEM model. Khan et al. [8] performed heat transfer analysis during SLM of AlSi10Mg alloy using adaptive remeshing technique to bring down the computational time and storage size. Fu et al. [2] examined the effects of process parameters on the melt pool geometry using FE model and validated the simulation results with experiments. Numerous models were developed to study the temperature profile but are limited to predict the temperature behavior with consideration of convective heat transfer inside the molten pool.

In the present work, the transient temperature field is predicted using a finite element model that is developed in the ABAQUS software. The model takes into account of all the heat losses by conduction, convection, radiation and also by convection inside the melt pool.

2 Methodology

2.1 Governing Equations for Heat Transfer Problem

The governing differential equation for a 3D heat transfer problem is given as

$$\rho c \frac{\partial T}{\partial t} = \frac{\partial}{\partial x}\left(k\frac{\partial T}{\partial x}\right) + \frac{\partial}{\partial y}\left(k\frac{\partial T}{\partial y}\right) + \frac{\partial}{\partial z}\left(k\frac{\partial T}{\partial z}\right) + Q \tag{1}$$

where ρ, c and k are the density, specific heat, and thermal conductivity of the material and Q is the internal heat generation. The boundary conditions are the convection and radiation heat transfer from the exposed surfaces which are given by the Eqs. (2) and (3)

$$Q_C = h(T - T_0) \tag{2}$$

$$Q_R = \sigma\varepsilon\left(T^4 - T_0^4\right) \tag{3}$$

To avoid the nonlinearity in the radiation term, an equivalent convective heat transfer coefficient is defined as $0.0024\ \varepsilon T^{1.61}$ with $\varepsilon = 0.35$. The related loss in accuracy is predicted to be less than 5% on using this term [9]. The initial temperature of the powder layer and the build platform is taken as 293 K.

2.2 Laser Energy Modeling

The laser energy is modeled by assuming it as a Gaussian surface heat flux which is symmetrical across the beam in terms of its irradiance [6]. The Gaussian heat flux for the fundamental mode (TEM_{00}) is given by

$$q(r) = \frac{2\alpha P}{\pi R^2} e^{-\frac{2r^2}{R^2}} \tag{4}$$

where P denotes laser power, R denotes radius of laser beam and α denotes absorptance of material which is taken as 0.1 [10]. The Gaussian heat flux is implemented using the DFLUX subroutine in ABAQUS [11].

2.3 Finite Element Modeling

The Finite element model consists of a single layer of powder and build platform as depicted in Fig. 1. The dimensions of the powder layer are 0.5 mm × 0.5 mm × 0.03 mm and are made of Ti6Al4V alloy. The dimensions of the build platform are 2 mm × 2 mm × 0.1 mm and are made of AISI steel. The geometry of the FE model is taken to be very small in size to reduce the computational time.

The powder layer is given as a fine mesh, whereas a coarser mesh is used for the build platform. An 8-noded hexahedral element (DC3D8) is used for the heat transfer analysis. Since latent heat effects are involved, a linear order element is used [12]. The thermal properties are given as a function of temperature and field variables for the powder layer [10]. The liquid's thermal conductivity is artificially enhanced to account for the convective heat transfer within the melt pool [9]. Field variable value 0 indicates powder state and field variable value 1 indicates solid/liquid state. By using the USDFLD subroutine [11], the field variable value is changed to 1 from 0 when the temperature at the integration point reaches above the melting point (i.e.1923 K). The simulation is performed for a single line laser scan track. The processing parameters used in the simulation process are given in Table 1. A tie constraint is used between the regions having dissimilar meshes [13]. The incrementation time is controlled by setting a value to the maximum allowable temperature change per increment.

3 Results and Discussion

The nodal temperatures obtained at the end of the simulation are shown in Fig. 2. The temperature distribution is analogous to the ones mentioned in the literature [7, 10]. The temperature is very high at the front end of the laser than at the rear end. This is due to the liquid's higher thermal conductivity than the powder, allowing improved heat transfer.

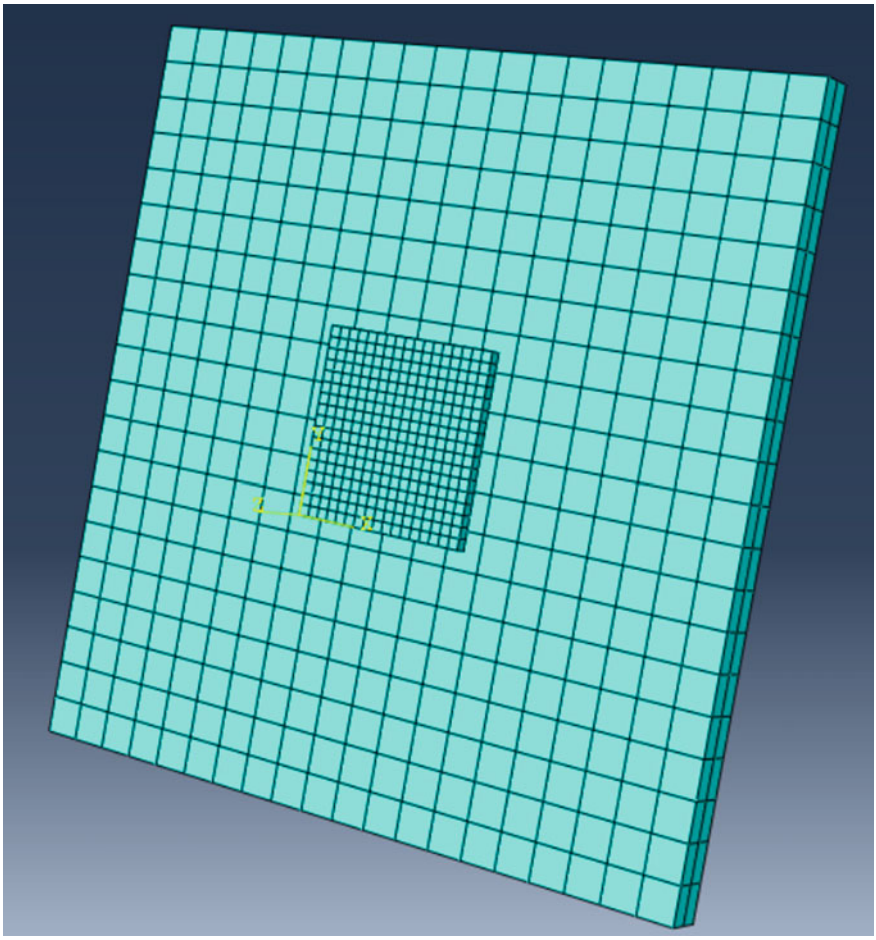

Fig. 1 Finite element model used in the simulation

Table 1 Process parameters for SLM of Ti6Al4V

Process parameters	Value
Powder layer thickness	0.03 mm
Laser power	140 W
Hatch spacing	0.1 mm
Scan speed	1.2 m/s
Laser spot size	0.1 mm

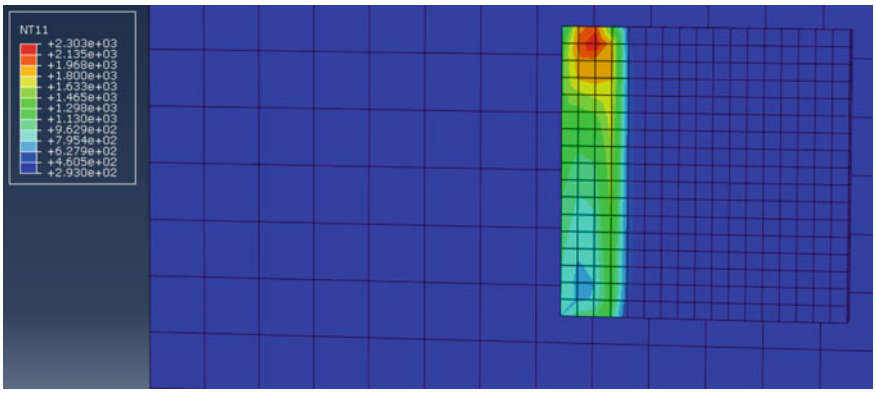

Fig. 2 Nodal temperatures obtained at the end of the simulation

The temperature–time history for a point on the surface of the powder layer is shown in Fig. 3. Once the laser beam approaches the point mentioned above, the temperature increases above the melting point to a value of around 2000 K. When the laser beam shifts forward, the temperature drops rapidly to around 750 K in a span of few milliseconds. Thus, it can be concluded that the temperature changes occur rapidly during the SLM process.

The variation of field variable with time is shown in Fig. 4, for the same point which was discussed earlier. The field variable becomes 1 when the temperature increases beyond 1923 K and this happens around 0.054 ms. After that, the field variable value remains 1 up to the end of the simulation indicating a solid/liquid state.

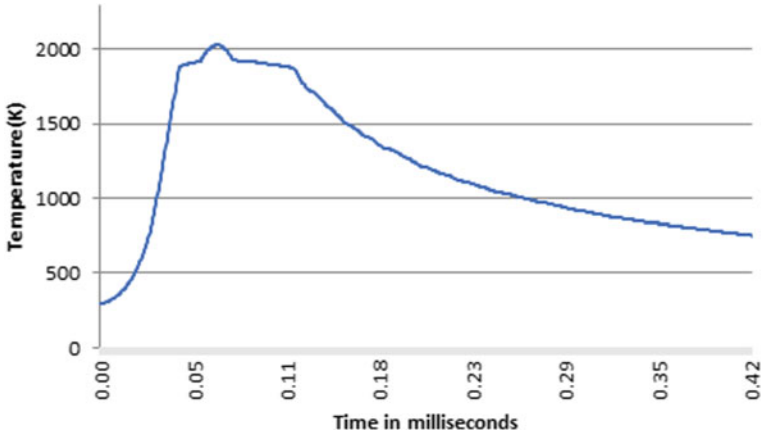

Fig. 3 Temperature–time history at a point on the powder layer surface

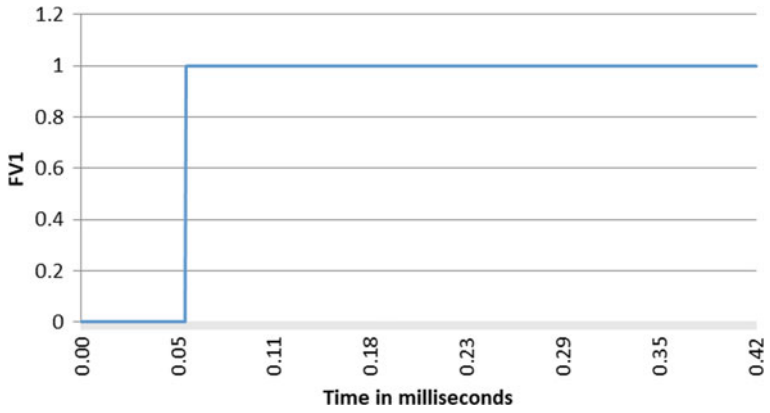

Fig. 4 Variation of field variable with time at a point

The field variables obtained at the end of the simulation are shown in Fig. 5. The red-colored region indicates the transformation of powder to solid-state, i.e., the solidified part and the unmelted regions shown in other colors. The unmelted regions can lead to part porosity. This defect could be avoided by either decreasing the scanning speed or increasing the laser power. Also, finer mesh could have reduced the region of unmelted powder.

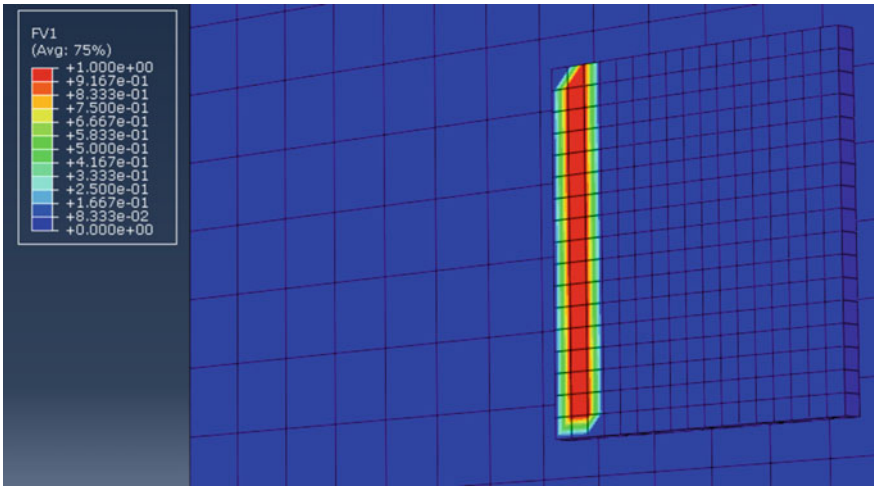

Fig. 5 Field variables representing the melted regions

4 Conclusion

A finite element model in 3D was developed in ABAQUS to obtain the temperature field for a single line laser scan track by considering the physical characteristics of the SLM process such as powder-liquid–solid phase transformation, temperature-dependent thermal properties, and accounting for all the heat transfer losses. The major findings are summarized below.

(1) The convection heat transfer which is taking place inside the melt pool is taken into account and the temperature field obtained is analogous to those mentioned in the literature.
(2) The developed model captured the rapid heating and cooling cycles involved in the SLM process which is solely culpable for the formation of residual stresses in the built part.
(3) The liquid's thermal conductivity had a great impact on the cooling rate of the melted portions of the powder layer
(4) The temperature near the front end of the laser is very high when compared to the region near the rear end of the laser.
(5) To estimate the residual stresses, the temperature field obtained using the heat transfer analysis can be used as a predefined field in the stress analysis.

References

1. Zaeh, M., Branner, G.: Investigations on residual stresses and deformations in selective laser melting. German Academic Society for Production Engineering (WGP) (2009)
2. Fu, C.H., Guo, Y.B.: Three-dimensional temperature gradient mechanism in selective laser melting of Ti-6AI-4V. J. Manuf. Sci. Eng., **136**(6), 061004 (2014)
3. Jamison, L., Bartlett, Li, X.: An overview of residual stresses in metal powder bed fusion. Additive Manuf. **27**, 131–149 (2019)
4. Kruth, J.P., Froyen, L., Van Vaerenbergh, J., Mercelis, P., Rombouts, M., Lauwers, B.: Selective laser melting of iron-based powders. J. Material Processing Tech. **149**, 616–622 (2004)
5. Bandyopadhyay, A., Traxel, K.D.: Metal-additive manufacturing—Modeling strategies for application-optimized designs. Addit. Manuf. **22**, 758–774 (2018)
6. Roberts, I.A., Wang, C.J., Esterlein, R., Stanford, M., Mynors, D.J.: A three-dimensional finite element analysis of the temperature field during laser melting of metal powders in additive layer manufacturing. Int. J. Mach. Tools Manuf **49**(12–13), 916–923 (2009)
7. Li, Y., Dongdong, Gu.: Parametric analysis of thermal behavior during selective laser melting additive manufacturing of aluminum alloy powder. Mater. Des. **63**, 856–867 (2014)
8. Khan, K., De, A.: Modelling of selective laser melting process with adaptive remeshing. Sci. Technol. Weld. Joining **24**, 391–400 (2019)
9. Liu, H.: Numerical analysis of thermal stress and deformation in the multi-layer laser metal deposition process. Masters Theses, 7242, (2014)
10. Sani: Selective Laser Melting process simulation: advancements towards a cost-effective model. Ph.D. thesis (2016)
11. Abaqus user subroutines reference manual (6.12), Dassault systems
12. Abaqus theory manual (6.12), Dassault systems
13. Abaqus Analysis user's manual (6.12), Dassault systems